

# Spectral diffusion and $^{14}\text{N}$ quadrupole splittings in absorption detected magnetic resonance hole burning spectra of photosynthetic reaction centers

J. W. Greis and A. Angerhofer<sup>a)</sup>

3 Physikalisches Institut, Universität Stuttgart, D 70550 Stuttgart, Germany

J. R. Norris

Chemistry Division, Argonne National Laboratory, Argonne, Illinois 60439

H. Scheer and A. Struck

Botanisches Institut, Universität München, Menzinger Strasse 67, D 80638 München, Germany

J. U. von Schütz

3 Physikalisches Institut, Universität Stuttgart, D 70550 Stuttgart, Germany

(Received 9 November 1993; accepted 20 December 1993)

Zero field absorption detected magnetic resonance hole burning measurements were performed on photosynthetic reaction centers of the bacteria *Rhodobacter sphaeroides* R26 and *Rhodospseudomonas viridis*. Extrapolation to zero microwave power yielded pseudohomogeneous linewidths of 2.0 MHz for *Rhodospseudomonas viridis*, 1.0 and 0.9 MHz for the protonated forms of *Rhodobacter sphaeroides* R26 with and without monomer bacteriochlorophyll exchanged, and 0.25 MHz as an upper limit for fully deuterated reaction centers of *Rhodobacter sphaeroides* R26. The measured linewidths were interpreted as being due to unresolved hyperfine interaction between the nuclear spins and the triplet electron spin, the line shape being determined by spectral diffusion among the nuclei. The difference in linewidths between *Rhodobacter sphaeroides* R26 and *Rhodospseudomonas viridis* is then explained by triplet delocalization on the special pair in the former, and localization on one dimer half on the latter. In the fully deuterated sample, four quadrupole satellites were observed in the hole spectra arising from the eight  $^{14}\text{N}$  nitrogens in the special pair. The quadrupole parameters seem to be very similar for all nitrogens and were determined to  $\kappa=1.25\pm 0.1$  MHz and  $\eta=0.9\pm 0.1$  MHz.

## I. INTRODUCTION

Optical detected magnetic resonance (ODMR) in zero external magnetic field has been used widely to study triplet excited states in various organic and inorganic molecules (see Refs. 1–3 and references therein). For triplet states in photosynthetic reaction centers (RCs), the absorption detection method (ADMR) has proven to be especially useful due to its improved sensitivity<sup>4–6</sup> over fluorescence detection magnetic resonance (FDMR) in the case of photosynthetic preparations with low fluorescence quantum yields.

ODMR hole burning and spin-echo experiments in zero field have been performed earlier on guest sites in molecular crystals to study the basic relaxation mechanisms of their triplet spins.<sup>7–9</sup> In many of these systems, transversal spin relaxation ( $T_2$ ) was found to be the result of spectral diffusion through fluctuating local fields caused by electron-phonon interactions with the lattice or by hyperfine coupling to the surrounding oscillating nuclear spins. Basic theoretical understanding of these mechanisms was developed by a number of workers<sup>10–13</sup> and later applied to the triplet spin with surrounding nuclear spins in chemically mixed crystals by van't Hof and Schmidt.<sup>9</sup> They found that spectral diffusion in these systems was caused by rapid, energy-

conserving spin flips of the nuclei interacting with the triplet spin. El-Sayed and co-workers measured the development of a burnt hole in the inhomogeneous triplet transition of traps in host-guest molecular crystals and demonstrated that the dynamic hole width is determined by the same spectral diffusion processes that are responsible for  $T_2$ .<sup>14,15</sup>

In photosynthetic systems, hole burning techniques have been applied mainly to distinguish different sites in the inhomogeneous ODMR line profile.<sup>16–21</sup> As for most isotropically diluted systems, the linewidths of the ADMR signals are inhomogeneously broadened due to small differences in the zero field splitting (zfs) values in different local environments (sites). Such site effects of the RC triplet state have been studied extensively by ODMR.<sup>4,17,18,20,22–29</sup>

The dynamic processes leading to transversal spin relaxation ( $T_2$ ) have received only little attention.<sup>30,31</sup> In particular, the correlation between the measured  $T_2$  and the hole widths is not very clear. Linewidths of 1–5 MHz have been reported for holes burnt in the ODMR transitions of various bacterial photosynthetic RCs<sup>16–18,20,21</sup> which seem to be too broad by at least a factor of 2 compared to the  $T_2=1.16\pm 0.05$   $\mu\text{s}$  determined by the ADMR spin-echo technique in the temperature range 1.2–2.1 K.<sup>31</sup> The Bloch equations<sup>32</sup>

$$\Delta\nu = 1/\pi T_2 \quad (1)$$

<sup>a)</sup>To whom correspondence should be addressed.

predicting ODMR hole widths of the order of 270 kHz using Lous'  $T_2$ .<sup>31</sup>

In order to clarify this apparent discrepancy and to gain a deeper understanding of the processes determining  $T_2$  and the ADMR hole widths, we have carried out rf power dependent ADMR hole burning experiments on RCs of *Rb. sphaeroides* R26 and *Rps. viridis* at 1.2 and 8 K.

## II. MATERIALS AND METHODS

Isolation of RCs from *Rb. sphaeroides* R26 and *Rps. viridis* was performed as described in Refs. 33–35. Pigment exchange with 3-vinyl-13<sup>2</sup>-OH-BChl *a* was performed as described earlier.<sup>36,37</sup> The deuterated sample of RCs from *Rb. sphaeroides* R26 was prepared according to Ref. 38. All samples were reduced with 50 mM sodium ascorbate at pH 8 as in Ref. 20 and diluted with 66% glycerol to form a clear glass on freezing. The optical density was adjusted to approximately 0.5 at 800 nm in a 2 mm quartz cuvette. The samples were illuminated while cooling with broadband light from the ADMR excitation lamp.

Our ADMR setup has previously been described.<sup>39</sup> For the hole burning and double resonance experiments, we used additional equipment.<sup>40</sup> The amplitude modulation frequency was set to 302 Hz.

Numerical calculations were performed on a HP 720 station using homewritten software.

## III. THEORY

### A. The ADMR hole burning experiment

Our ADMR experiment is described in the frame of the four-level model<sup>39,41</sup> in which only the singlet ground state and the three triplet sublevels are considered because of the negligible stationary population of higher excited states. Neglecting spin-lattice relaxation (SLR), which is reasonable at very low temperatures, the rate equations for the populations of the singlet ground state ( $S_0$ ) and the three triplet sublevels ( $\tau_i$ ) ( $i = x, y, z$ ) are

$$\frac{d}{dt} (S_0) = -A(S_0) + \sum_{i=x}^z k_i(\tau_i), \quad (2)$$

$$\begin{aligned} \frac{d}{dt} (\tau_x) = & p_x A(S_0) - k_x(\tau_x) - s[(\tau_x) - (\tau_z)] \\ & - q[(\tau_x) - (\tau_y)], \end{aligned} \quad (3)$$

$$\begin{aligned} \frac{d}{dt} (\tau_y) = & p_y A(S_0) - k_y(\tau_y) - r[(\tau_y) - (\tau_z)] \\ & - q[(\tau_y) - (\tau_x)], \end{aligned} \quad (4)$$

$$\begin{aligned} \frac{d}{dt} (\tau_z) = & p_z A(S_0) - k_z(\tau_z) - r[(\tau_z) - (\tau_y)] - s[(\tau_z) - (\tau_x)] \end{aligned} \quad (5)$$

with the rf transition rates  $q$ ,  $r$ , and  $s$  in the  $2|E|$ ,  $|D| - |E|$ , and  $|D| + |E|$  transitions,  $A$  is the light excitation rate, and  $p_i$  and  $k_i$  ( $i = x, y, z$ ) are the triplet sublevel population probabilities and decay rates. The signal intensities of the cw-

ADMR experiment are evaluated by considering only the stationary solution of this system of four differential equations. For example, for the  $|D| - |E|$  signal, the intensity is given by<sup>42,43</sup>

$$I_{\text{ADMR}} = \frac{\Delta I}{I} = \sum_{i=x}^z \{[\tau_i(r)] - [\tau_i(0)]\} = \frac{r}{h + (r/A_\infty)} \quad (6)$$

with

$$A_\infty = \frac{k_x k_y k_z}{b} - \frac{k_x k_y + k_x k_z}{a}, \quad (7)$$

$$a = -2k_x A(p_y + p_z) - p_x A(k_y + k_z) - k_x(k_y + k_z), \quad (8)$$

$$b = -A k_y(k_x p_z + k_z p_x) - A k_x k_z p_y - k_x k_y k_z, \quad (9)$$

$$h = b/aA_\infty, \quad (10)$$

where  $I$  is the intensity of the light transmitted through the sample.

In the case of hole burning experiments, two rf frequencies are applied separately to the sample. The hole burning frequency  $\nu_1$  is kept fixed at the desired value somewhere within the inhomogeneous transition under study, and is amplitude modulated. This way of performing the experiment assures that only the burnt hole, and possibly correlated double resonance signals, are being observed upon sweeping the probe frequency  $\nu_2$  through the transition. The stationary baseline is shifted by the amount of the ADMR signal caused by the fixed frequency. The transition rates of the two rf signals in the triplet system follow a Lorentzian frequency distribution

$$r_j(\nu_j) = \frac{a_j \Delta \nu}{\Delta \nu^2 + 4(\nu_j - \nu_S)^2} \quad \text{with} \quad \int_{-\infty}^{\infty} r_j(\nu_j) d\nu_j = r_{0j} \quad (11)$$

with  $\nu_j$  ( $j = 1$  and  $2$ ) the fixed and swept frequencies,  $\nu_S$  is the resonance frequency of a given site, and  $\Delta \nu$  is its pure lifetime-limited linewidth.  $a_j$  stands for the amplitudes of the transition rates which are proportional to the applied rf power in the low power limit (Fermi's golden rule). The ADMR hole spectrum is found by modulating the fixed frequency  $\nu_1$  and constantly applying and sweeping frequency  $\nu_2$  over the desired range. The corresponding hole signal is given by Eq. (6)<sup>42</sup>

$$I_{\text{hole}} = \sum_{i=x}^z [\tau_i(r_1 + r_2) - \tau_i(r_2)] = \frac{A_\infty^2 h r_1}{(A_\infty h + r_2)^2 + (A_\infty h + r_2) r_1} \quad (12)$$

with the parameters as defined in Eqs. (7)–(10).

Inserting Eq. (11) for  $r_1$  and  $r_2$  in this expression gives the signal for a hole burning experiment on a homogeneous line centered at  $\nu_S$ . In the case of an inhomogeneously broadened line, the resonance frequencies obey a Gaussian distribution

$$g(\nu_S - \nu_0) = \frac{2}{\Delta\nu_G} \sqrt{\frac{\ln 2}{\pi}} \exp\left[-\frac{4 \ln(2)(\nu_S - \nu_0)^2}{\Delta\nu_G^2}\right] \quad (13)$$

with  $\nu_0$  and  $\Delta\nu_G$  the center and width of the Gaussian distribution and the normalization condition

$$\int_{-\infty}^{\infty} g(\nu_S - \nu_0) d\nu_S = 1. \quad (14)$$

We can now calculate the hole signal by integrating over the whole inhomogeneous line which includes all possible sites with their Gaussian statistical weights

$$I_{\text{hole}}(\nu_1, \nu_2) = c a_1 \Delta\nu^2 \int_{-\infty}^{\infty} \frac{(A_\infty h + \{(a_2 \Delta\nu)/[\Delta\nu^2 + 4(\nu_2 - \nu_S)^2]\})^{-2} \exp\{-4 \ln(2)(\nu_S - \nu_0)^2/\Delta\nu_G^2\}}{\Delta\nu^2 + \Delta\nu a_1 (A_\infty h + \{(a_2 \Delta\nu)/[\Delta\nu^2 + 4(\nu_2 - \nu_S)^2]\})^{-1} + 4(\nu_1 - \nu_S)^2} d\nu_S \quad (15)$$

with

$$c = \frac{2}{\Delta\nu_G} \sqrt{\frac{\ln(2)}{\pi}} A_\infty^2 h. \quad (16)$$

Equation (15) represents the intensity at one single point of the hole burning spectrum. To get the whole spectrum, one has to sweep  $\nu_2$  through the desired range and calculate Eq. (15) for each data point. For the simulation of the spectra,  $\nu_0$  was determined from the ADMR experiment, the light excitation rate was determined from bleaching experiments using unreduced RCs, or calculated using the known light flux of the lamp and the optical density of the sample. All other triplet state parameters were taken from the literature.<sup>5,39</sup> The only remaining unknown parameters are the pseudohomogeneous linewidth and the proportionality factor connecting the transition rates  $a_j$  for the three triplet sublevel transitions with the applied rf power. The latter was obtained by fitting the calculated hole width with the experimental data in the region where power broadening was observed. The homogeneous linewidth was obtained by variation of  $\Delta\nu$  in Eq. (15), fitting the calculated data with the experimental hole widths at very low rf powers where power broadening was not observed anymore. The linewidths gained this way are approximately half the experimental hole widths extrapolated to zero rf power.

## B. Estimation of the hyperfine interaction in zero field

In zero field, hyperfine interaction is operative only in second order of perturbation theory. For the estimation of the expected effect, we follow the arguments of Hutchison *et al.*<sup>44</sup> in the limit of what they call the "almost-zero-field range." For a rather crude first approximation, we only consider isotropic hyperfine interaction in our perturbation Hamiltonian

$$\hat{H}_{\text{pert}} = \sum_k a_k \mathbf{S} \mathbf{I}_k. \quad (17)$$

The unperturbed Hamiltonian contains the dipole-dipole interaction of the two triplet electrons. The perturbation (17) creates an energy shift for a given constellation of nuclear spins. Different constellations of the nuclei (more than one is required) cause level splittings of the triplet sublevels and thereby shifts in the corresponding transition frequencies (which is the difference between two connected triplet sub-

level energies). In the presence of many nuclei with different hyperfine constants  $a_k$ , these frequency shifts smear out into an unresolved line shape. The width of this line shape is determined by the standard deviation  $\sigma_A$  (second moment) of the averaged hyperfine interaction  $\langle A^2 \rangle$

$$\langle A^2 \rangle = \sum_k (a_k I_k)^2, \quad (18)$$

$$\sigma_A = \sqrt{\frac{\sum_{p=1}^N (A_p^2 - \langle A^2 \rangle)^2}{N-1}}. \quad (19)$$

We have to take the square of the hyperfine interaction since at zero field the perturbation in first order is zero. If the hyperfine interaction at all three zero-field transitions is equal, we can write the hyperfine induced broadenings as<sup>9,44</sup>

$$h\Delta\nu_{|D|+|E|} = \left( \frac{1}{2|E|} + \frac{1}{|D|-|E|} + \frac{2}{|D|+|E|} \right) 2\sigma_A^2, \quad (20)$$

$$h\Delta\nu_{|D|-|E|} = \left( \frac{1}{2|E|} + \frac{2}{|D|-|E|} + \frac{1}{|D|+|E|} \right) 2\sigma_A^2, \quad (21)$$

$$h\Delta\nu_{2|E|} = \left( \frac{2}{2|E|} + \frac{1}{|D|-|E|} + \frac{1}{|D|+|E|} \right) 2\sigma_A^2. \quad (22)$$

## C. Spectral diffusion

Since the linewidths estimated in Eqs. (20)–(22) are composed of the contributions of many different hyperfine constellations, they constitute an inhomogeneous line. If spectral diffusion by fast (on the time scale of the experiment) fluctuations of these hyperfine constellations takes place, these lines cannot be resolved anymore by the hole burning experiment. The whole line will be burnt as if it were homogeneous, with its linewidth determined by the distribution of hyperfine interactions given in Eqs. (20)–(22). The line has become pseudohomogeneous with a so-called static linewidth. However, in the case of a time-resolved experiment, the apparent linewidth may decrease if the experiment is done on a time scale comparable or faster than the nuclear fluctuations.<sup>14,15</sup> This is then called a dynamic linewidth. The  $T_2$  times derived from a spin-echo experiment may then reflect the characteristic times of the nuclear flip-flop processes<sup>9,10</sup> if there are no other dephasing processes.

Fast spin exchange among the nuclei is thus responsible for the spectral diffusion of the triplet sublevel transitions, i.e., the hopping of the triplet transition frequencies within the distribution defined by the hyperfine (and quadrupole) interactions, which in turn causes the transversal relaxation of the electron spin. Hu and Hartmann<sup>10</sup> derived an expression for the amplitude of a spin echo  $E(t)$  depending on the linewidth  $\Delta\omega$ ,

$$E(t) = \exp[-\frac{1}{2}\Delta\omega K(Wt)t], \quad (23)$$

where  $W$  is the total flip-flop rate of the nuclear spins.  $K(Wt)$  can only be calculated numerically and is listed for different parameters  $Wt$  in Ref. 10. It is remarkable that the decay is nonexponential, but can be approximated exponentially for special time domains (this would be necessary for the definition of  $T_2$ ). Of special interest is the limit where  $K(Wt)$  reaches its maximum value. In that case, the spin-echo decay comes very close to an exponential decay and can be approximated by<sup>10</sup>

$$E_{\text{limit}}(t) = \exp[-(\Delta\omega t)/(2\sqrt[3]{\pi})]. \quad (24)$$

This translates into a relation between the static linewidth  $\Delta\nu$  and an apparent  $T_2$  observable from a monoexponential fit in a spin-echo decay experiment, of

$$\frac{1}{T_2} = \frac{\Delta\omega}{2\sqrt[3]{\pi}}. \quad (25)$$

This limit is applicable when the average spin-flip rate  $W$  is approximately equal to half the static linewidth  $\Delta\nu$ . Although the flip rate of two adjacent nuclear spins is within the order of their dipolar interaction ( $\approx 10$  kHz), the average flip rate due to many nuclear spins interacting with the electron spin  $S$  can be much higher, reaching the order of the measured  $T_2^{-1}$  values. If nuclear spin diffusion is the dominant process for triplet spin relaxation in our case, we can estimate the apparent  $T_2$  by measuring the linewidths of the ADMR holes.

Temperature dependent relaxation effects don't have to be considered here because we did not detect any changes in the measured hole widths between 1.2 and 8 K.

#### D. Quadrupole splittings

The quadrupole effect needs a more precise examination since we find satellite lines at high rf powers. When a simultaneous spin flip of an electron spin and a nuclear  $I=1$  spin occurs, the transition frequency shifts by the amount of the quadrupole energy. If this shift is of the order of the homogeneous linewidth, it will cause additional broadening of the holes; if it is larger, one can observe discrete lines separated from the hole center by the quadrupole energy (satellite lines). Since these flip-flop processes are spin forbidden, they are only visible at very high rf power.<sup>45,46</sup>

In zero magnetic field, the quadrupole splitting is given by

$$\hat{H}_Q = \kappa[3I_z^2 - I^2 + \eta(I_x^2 - I_y^2)] \quad (26)$$

with the asymmetry parameter  $\eta$  and

$$\kappa = \frac{e^2 Q q}{4h} \quad (27)$$

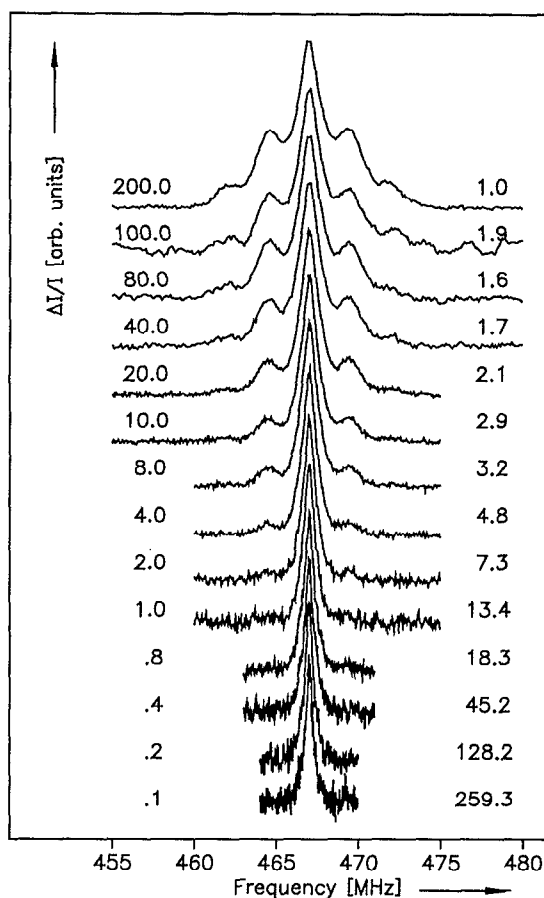


FIG. 1. Power dependent ADMR hole burning spectra of deuterated RCs of *Rb. sphaeroides* R26 at the  $|D\rangle - |E\rangle$  transition at 8 K. The hole burning frequency was set to 467 MHz. All spectra are normalized to equal height. The normalization factors for each spectrum are indicated on the right; the applied rf power of both rf frequencies on the left.

( $Q$ =quadrupole moment and  $eq$ =field gradient in the  $z$  direction). The resulting shifts in the transition frequencies are

$$h\Delta\nu_{q1} = 2\kappa\eta, \quad (28)$$

$$h\Delta\nu_{q2} = \kappa(3 - \eta), \quad (29)$$

$$h\Delta\nu_{q3} = \kappa(3 + \eta). \quad (30)$$

#### IV. RESULTS

Typical power dependent ADMR hole burning spectra are shown in Fig. 1 for the  $|D\rangle - |E\rangle$  signal of the triplet state in deuterated RCs of *Rb. sphaeroides* R26. At low rf powers, the signals are rather weak and very narrow ( $\sim 0.25$  MHz FWHM). As the power increases, one observes an increase in signal intensity as well as in linewidth (power broadening). The hole burning frequency was set to 467 MHz on the  $|D\rangle - |E\rangle$ -signal. At high rf powers, one can observe four nuclear quadrupole satellites at equal distances of 2.4 and 4.9 MHz above and below the hole burning frequency. The holes detected on the other two triplet transitions ( $|D\rangle + |E\rangle$  and  $2|E\rangle$ ) were identical to those shown in Fig. 1.

Figure 2 shows the power dependence of the hole widths of four different RC preparations—deuterated RCs of *Rb.*

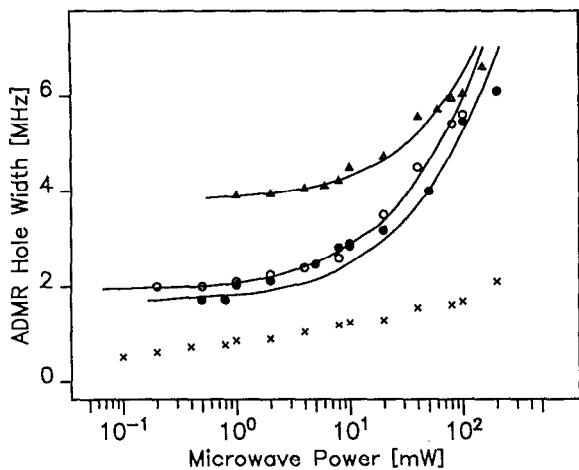


FIG. 2. Power dependence of the measured ADMR hole widths at 8 K of RCs of *Rps. viridis* ( $\Delta$ ), *Rb. sphaeroides* R26 ( $\bullet$ ), *Rb. sphaeroides* R26 with their BChl monomers exchanged by 3-vinyl-13<sup>2</sup>-OH-BChl *a* ( $\circ$ ), and deuterated *Rb. sphaeroides* R26 ( $\times$ ). Experimental error is about twice the size of the symbols. Theoretical fits (lines through the data points) for the unmodified and modified RCs of *Rb. sphaeroides* R26 and *Rps. viridis* yield 2.0 ( $\Delta$ ), 0.9 ( $\bullet$ ), and 1.0 MHz ( $\circ$ ), and an upper limit of 0.25 MHz ( $\times$ ).

*sphaeroides* R26, protonated RCs of *Rb. sphaeroides* R26, RCs with modified BChl monomers (*Rb. sphaeroides* R26), and RCs of *Rps. viridis*. For the protonated species, the power broadening region begins above about 10 mW of applied rf power. At lower powers, the linewidths are nearly constant and can be extrapolated to zero rf power. This is done by numerically fitting the power dependence as described in the Theory section and shown in Fig. 2 by the lines through the data points, yielding  $\Delta\nu < 0.25, 1.0, 0.9,$  and 2.0 MHz for the four samples. In the case of the deuterated sample, power broadening is still visible at the lowest applied rf power of 100  $\mu$ W. Below this rf power, the signals are not detectable with our setup. It is therefore difficult to fit the theoretical curve with two free parameters to these data points, which allows only to define an upper limit of 0.25 MHz for the homogeneous linewidth.

## V. DISCUSSION

### A. The pseudohomogeneous linewidth

Since the linewidth is remarkably reduced by deuteration, we conclude that unresolved hyperfine interaction is responsible for the observed hole widths.

The expected linewidths can be estimated from the standard deviation of the hyperfine broadening in second order perturbation theory [see Eqs. (20)–(22)]. The relevant hyperfine coupling constants are taken from the literature.<sup>47,48</sup> For the four nitrogens of one BChl in the dimer,  $a_n = 1.43, 1.43, 1.25,$  and 1.0 MHz; for the protonated RCs, only five protons with the largest hyperfine couplings were taken into account (four  $\beta$  protons and one  $\alpha$  proton) with coupling constants of  $|a_p| = 4.5, 4.5, 2.8, 2.8,$  and 2.7 MHz.

Using Eq. (18), we then estimate an average hyperfine interaction of 0.5 MHz and its corresponding second moment from Eqs. (20)–(22) to 1.0 MHz. According to Eq. (15), this

would predict a minimal hole width of approximately 2.0 MHz, which is exactly what we find for the two protonated RCs of *Rb. sphaeroides* R26. The very small difference in homogeneous linewidths between normal RCs (0.9 MHz) and those modified at the BChl monomer positions (1.0 MHz) shows that there is very little influence of the neighboring molecules on the triplet state spin density on the primary donor. This has also been found previously to be the case in ENDOR studies where the spin densities of the primary donor cation were not changed by modification of the monomeric BChls.<sup>49</sup>

This estimation is based on the concept that in *Rb. sphaeroides* R26, the triplet state is delocalized equally over both dimer halves.<sup>50</sup> A different situation has been suggested for the RC from *Rps. viridis*, where the extreme case of complete localization on one BChl of the dimer may have to be considered.<sup>50,51</sup> We take this into account by including only the nuclei of one dimer half (half the number of nuclei) with their coupling constants doubled. This yields a second moment of the order of 2.0 MHz, twice as large as in the delocalized case. For this rather crude first order approximation, we assume that the geometries of the primary donors of *Rb. sphaeroides* R26 and *Rps. viridis* are comparable and that the corresponding hyperfine interactions differ by a factor of 2 due to the localization of the triplet on one dimer half in *Rps. viridis*. This assumption seems to be justified from the differences in the dimer structure between both organisms observed by x-ray crystallography, and triplet electron paramagnetic resonance (EPR) and ADMR.<sup>50–52</sup>

We therefore predict a homogeneous linewidth of about 2.0 MHz for *Rps. viridis*, which agrees well with the observed one. This is further evidence that the triplet state is localized mainly on one BChl of the dimer in *Rps. viridis*.

Recent electron spin echo envelope modulation (ESEEM) and single crystal electron nuclear double resonance (ENDOR) data indicate that the delocalization of the wave function of the primary donor cation is asymmetric with a ratio of 2:1 for the spin densities on the *A* vs *B* parts of the primary donor of both *Rb. sphaeroides* R26 and *Rps. viridis*.<sup>53–58</sup> This is surprising because the extent of delocalization of both triplet and cation wave functions should in principle be governed by the same type of nuclear overlap integrals.<sup>59</sup> Differences in delocalization between the triplet and the cation wave functions may then be the result of slight differences in dimer geometry due to the extra charge in the cation. In view of these differences, we can compare the second moments of our ADMR holes only with the previously published triplet EPR and ADMR data.

In the case of the deuterated RCs of *Rb. sphaeroides* R26, the deuterium hyperfine coupling constants can be neglected since they are smaller by a factor of 6.5, which scales to about 16 in second order perturbation theory. Using the remaining nitrogen hyperfine couplings, the delocalized triplet state yields an average hyperfine interaction of 0.1 MHz and its standard deviation of 0.1 MHz, which predicts a homogeneous linewidth of about 0.2 MHz. The experimental upper limit for the linewidth of 0.25 MHz agrees with this estimation. From the excellent agreement between calculated hyperfine broadening and experimental hole widths in all

four cases, we conclude that unresolved hyperfine interaction is responsible for the hole widths.

In our cw experiment, the measured hole widths are due to spectral diffusion within the hyperfine broadened transition at any given site of the magnetically dilute system. Since variation of the temperature does not play a role in our experiments (between 1.2 and 8 K) and in those of Lous *et al.*<sup>31</sup> (between 1.2 and 2.1 K), this spectral diffusion process must be caused by energy-conserving spin exchange reactions among the nuclei coupled to the triplet system by hyperfine interaction.<sup>9,10</sup> The average rate at which these nuclear flip-flop processes take place determines the rate of spin diffusion and distinguishes between static and dynamic linewidths.

If the hole burning experiments were done time resolved, the spins would not have enough time to diffuse within the hyperfine-defined linewidth. The measured hole width would decrease from its static value to a dynamic linewidth, as demonstrated by El-Sayed and co-workers to be the case in mixed organic crystals.<sup>14,15</sup>

The difference between static and dynamic linewidths is probably the reason for the apparent discrepancy between the  $T_2$  of  $1.16 \pm 0.05 \mu\text{s}$  measured by Lous *et al.*<sup>31</sup> and that calculated from the ODMR linewidths using Eq. (1). The spin-echo experiment employed by Lous is a time-resolved method that samples only part of the spectral distribution, consequently leading to an apparently longer  $T_2$  than calculated from the static linewidth using the ordinary Bloch equation approach. According to the theory by Hu and Hartmann,<sup>10</sup> the spin-echo signal amplitude in this case is no longer monoexponential (with a given  $T_2$ ) as expected from the Bloch equations,<sup>32</sup> but rather a complex function of the nuclear spin-flip rate and time [see Eq. (23)]. If we take Eq. (24) as the lower limit of a spin-echo decay experiment, the data from the hole burning and spin-echo experiments match perfectly. Inserting our measured linewidths of 900 kHz for the RCs of *Rb. sphaeroides* R26 in Eq. (25), we arrive at an apparent  $T_2$  of  $1.04 \mu\text{s}$ , very close to Lous' data. The limit in which Eq. (25) is best approached is when the function  $K(Wt)$  (tabulated in Ref. 10) reaches its maximum value, i.e., when the spin-flip rate is approximately equal to half the static linewidth. For the protonated samples of *Rb. sphaeroides* R26, this is of the order of 500 kHz.

## B. Quadrupole satellites

At rf powers higher than 10 mW, quadrupole satellites of the  $^{14}\text{N}$  nuclei were observed in deuterated RCs of *Rb. sphaeroides* R26 (see Figs. 1 and 3). The resonance frequencies of these satellites are given by the correlation

$$\nu = \nu_h \pm \nu_N. \quad (31)$$

According to Eqs. (28)–(30), one should observe three additional satellite lines for each nitrogen nucleus at both sides of the hole center frequency  $\nu_h$ . Instead of 48 lines expected for the eight nitrogens of the dimer, we only observe four, two on either side. This may be explained by assuming that all eight nitrogens experience similar electric field gradients resulting in similar quadrupole splittings, and that two transitions overlap having thus twice the intensity of the third one.

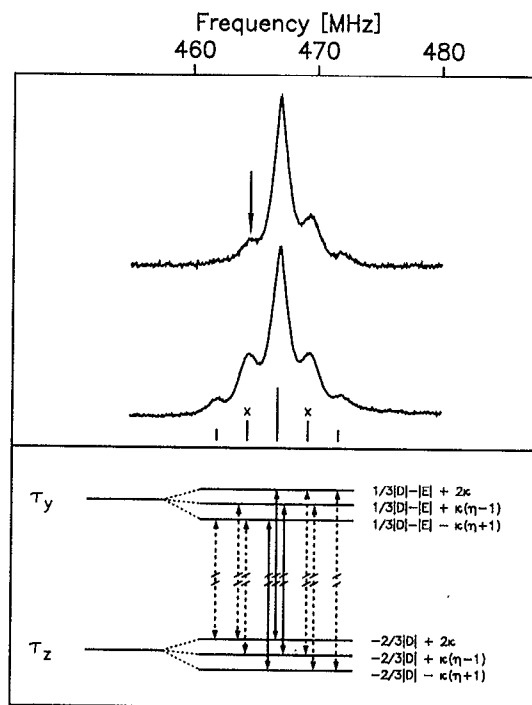


FIG. 3. ADMR hole burnt in the  $|D|-|E|$  transition of deuterated RCs of *Rb. sphaeroides* R26 at 8 K and 200 mW of rf power for both the fixed and swept frequencies (lower spectrum). The interpretation of the nuclear quadrupole satellites is indicated by the level diagram. The satellite lines on one side of the hole can be burnt by an additional rf frequency, indicated by the arrow in the upper spectrum.

This assumption is strengthened by the observation that all satellite bands on one side of the hole can be burned by applying an additional rf frequency fixed on one of these lines (see the upper spectrum in Fig. 3 with the arrow indicating the additional rf frequency used to burn the quadrupole lines). Due to the very slow relaxation between the nuclear quadrupole levels at low temperatures, the transitions can be saturated easily in a stationary experiment.<sup>45,46</sup> Further resolution of additional quadrupole lines possibly hidden under the spectrum was not obtained by this “triple resonance” experiment. If this interpretation of the quadrupole satellites is correct, we arrive at parameters of  $\kappa = 1.25 \pm 0.1$  MHz and  $\eta = 0.9 \pm 0.1$  MHz.

In contrast to these results, de Groot *et al.* arrived at different quadrupole parameters from their ESEEM data taken in the X band.<sup>48</sup> Their range of values ( $0.77$ – $1.14$  MHz for  $\kappa$  and  $0.18$ – $0.80$  MHz for  $\eta$ ) were derived under the assumption that the anisotropic hyperfine interaction can be neglected with respect to the quadrupole interaction, and that the observed modulations arise from those electron spin orientations where isotropic hyperfine interaction approximately cancels the nuclear Zeeman interaction. Such assumptions may be considered in certain systems and, where applicable, facilitate the interpretation of ESEEM spectra considerably.<sup>60</sup> However, if de Groot's analysis were valid in the present case, we should not observe the relatively large splittings between the hole and the satellite lines. The latter should lie closer to the hole frequency and probably not even be resolvable any more. This clearly indicates that the as-

sumptions of de Groot *et al.* in interpreting the ESEEM data are not justified.

No such assumptions are necessary in our analysis because the contributions of the nuclear Zeeman interaction are orders of magnitude smaller in zero field (compared to the  $X$ -band field), and anisotropic hyperfine interaction may only contribute to the second moment, but cannot induce a splitting like the observed satellite pattern.

## VI. CONCLUSIONS

We have demonstrated that the linewidth in ADMR hole burning experiments is caused by unresolved hyperfine interaction in second order perturbation theory. The agreement between experimental and calculated linewidths confirms the concept of the triplet state being delocalized in *Rb. sphaeroides* R26 and mainly localized in *Rps. viridis*. Modification of the BChl accessory monomers shows negligible effects on the hole widths.

Assuming temperature independent spectral diffusion within the hyperfine broadened line, the apparent disagreement between the measured hole widths and the  $T_2$ 's derived by Lous *et al.*<sup>31</sup> with spin-echo techniques could be resolved.

Quadrupole resonance is observed by satellite lines of the holes in deuterated RCs. Our results show that values for the quadrupole parameters  $\kappa$  and  $\eta$  derived earlier from ESEEM in  $X$  band<sup>48</sup> have to be corrected.

## ACKNOWLEDGMENTS

We would like to thank Professor H. C. Wolf for his interest and support. The work in Stuttgart was supported by the Deutsche Forschungsgemeinschaft. The work in München was supported by the Deutsche Forschungsgemeinschaft under project A9 of the Sonderforschungsbereich "Elementarprozesse der Photosynthese." The fully deuterated RCs of *Rb. sphaeroides* R26 were prepared by Ursula Smith at Argonne National Laboratory with financial support by the Department of Energy under Contract No. W-31-109-Eng-38. J.R.N. gratefully acknowledges support from the Alexander von Humboldt foundation.

<sup>1</sup> *Triplet State ODMR Spectroscopy*, edited by R. H. Clarke (Wiley, New York, 1982).

<sup>2</sup> A. L. Kamyshny, A. P. Suisalu, and L. A. Aslanov, *Coord. Chem. Rev.* **117**, 1 (1992).

<sup>3</sup> A. Angerhofer, in *The Chlorophylls*, edited by H. Scheer (CRC, Boca Raton, FL, 1991), p. 945.

<sup>4</sup> H. J. den Blanken, G. P. van der Zwet, and A. J. Hoff, *Chem. Phys. Lett.* **85**, 335 (1982).

<sup>5</sup> H. J. den Blanken and A. J. Hoff, *Biochim. Biophys. Acta* **681**, 365 (1982).

<sup>6</sup> J. Ullrich, A. Angerhofer, J. U. von Schütz, and H. C. Wolf, *Chem. Phys. Lett.* **140**, 416 (1987).

<sup>7</sup> J. Schmidt, *Chem. Phys. Lett.* **14**, 411 (1972).

<sup>8</sup> W. G. Breiland, H. C. Brenner, and C. B. Harris, *J. Chem. Phys.* **62**, 3458 (1975).

<sup>9</sup> C. A. van't Hof and J. Schmidt, *Mol. Phys.* **38**, 309 (1979).

<sup>10</sup> P. Hu and S. R. Hartmann, *Phys. Rev. B* **9**, 1 (1974).

<sup>11</sup> J. R. Klauder and P. W. Anderson, *Phys. Rev.* **125**, 912 (1962).

<sup>12</sup> W. B. Mims, K. Nassau, and J. D. McGee, *Phys. Rev.* **123**, 2059 (1961).

<sup>13</sup> W. B. Mims, *Phys. Rev.* **168**, 370 (1968).

<sup>14</sup> W. M. Pitts and M. A. El-Sayed, *Mol. Cryst. Liq. Cryst.* **58**, 19 (1980).

<sup>15</sup> A. R. Burns, M. A. El-Sayed, and J. C. Brock, *Chem. Phys. Lett.* **75**, 31 (1980).

<sup>16</sup> R. H. Clarke and R. E. Connors, *Chem. Phys. Lett.* **42**, 69 (1976).

<sup>17</sup> A. J. Hoff, *Biochim. Biophys. Acta* **440**, 765 (1976).

<sup>18</sup> J. Beck, J. U. von Schütz, and H. C. Wolf, *Chem. Phys. Lett.* **94**, 141 (1983).

<sup>19</sup> J. Beck, J. U. von Schütz, and H. C. Wolf, *Z. Naturforsch. Teil C* **38**, 220 (1983).

<sup>20</sup> A. Angerhofer, J. U. von Schütz, and H. C. Wolf, *Z. Naturforsch. Teil C* **39**, 1085 (1984).

<sup>21</sup> J. Greis, A. Angerhofer, R. Speer, J. U. von Schütz, J. Ullrich, and H. C. Wolf, in *Current Research in Photosynthesis, Proceedings of the VIIIth International Conference on Photosynthesis, Stockholm, Sweden, August 6-11, 1989*, edited by M. Baltscheffsky (Kluwer, Dordrecht, 1990), Vol. 1, p. 1.145.

<sup>22</sup> H. J. den Blanken, G. P. van der Zwet, and A. J. Hoff, *Biochim. Biophys. Acta* **681**, 375 (1982).

<sup>23</sup> A. J. Hoff and H. G. de Vries, *Isr. J. Chem.* **21**, 277 (1981).

<sup>24</sup> H. J. den Blanken, A. P. J. M. Jongenelis, and A. J. Hoff, *Biochim. Biophys. Acta* **725**, 472 (1983).

<sup>25</sup> H. J. den Blanken, H. Vasmel, A. P. J. M. Jongenelis, A. J. Hoff, and J. Ames, *FEBS Lett.* **161**, 185 (1983).

<sup>26</sup> H. J. den Blanken and A. J. Hoff, *Chem. Phys. Lett.* **98**, 255 (1983).

<sup>27</sup> A. J. Hoff, H. J. den Blanken, H. Vasmel, and R. F. Meiburg, *Biochim. Biophys. Acta* **806**, 389 (1985).

<sup>28</sup> R. van der Vos, P. J. van Leeuwen, P. Braun, and A. J. Hoff, *Biochim. Biophys. Acta* **1140**, 184 (1992).

<sup>29</sup> A. J. Hoff, NATO ASI Ser. A **149**, 89 (1988); Proceedings of a NATO Advanced Research Workshop on the Structure of the Photosynthetic Bacterial Reaction Center, held September 20-25, 1987 at the Centre d'Etudes Nucléaires de Cadarache, France.

<sup>30</sup> N. Nishi, J. Schmidt, A. J. Hoff, and J. H. van der Waals, *Chem. Phys. Lett.* **56**, 205 (1978).

<sup>31</sup> E. J. Lous and A. J. Hoff, *Chem. Phys. Lett.* **140**, 620 (1987).

<sup>32</sup> A. Carrington and A. D. McLachlan, *Introduction to Magnetic Resonance* (Harper & Row, New York, 1969).

<sup>33</sup> G. Feher and M. Y. Okamura, in *The Photosynthetic Bacteria*, edited by R. K. Clayton and W. R. Sistrom (Plenum, New York, 1978), p. 349.

<sup>34</sup> D. Beese, R. Steiner, H. Scheer, A. Angerhofer, B. Robert, and M. Lutz, *Photochem. Photobiol.* **47**, 293 (1988).

<sup>35</sup> J. P. Thornber, R. J. Cogdell, R. E. B. Seftor, and G. D. Webster, *Biochim. Biophys. Acta* **593**, 60 (1980).

<sup>36</sup> A. Struck, E. Cmiel, I. Katheder, and H. Scheer, *FEBS Lett.* **268**, 180 (1990).

<sup>37</sup> A. Struck and H. Scheer, *FEBS Lett.* **261**, 385 (1990).

<sup>38</sup> C. A. Wraight, *Biochim. Biophys. Acta* **548**, 309 (1979).

<sup>39</sup> A. Angerhofer, R. Speer, J. Ullrich, J. U. von Schütz, and H. C. Wolf, *Appl. Magn. Reson.* **2**, 203 (1991).

<sup>40</sup> A. Angerhofer, G. Friso, G. M. Giacometti, and G. Giacometti, *Biochim. Biophys. Acta* (to be published).

<sup>41</sup> A. J. Hoff and B. Cornelissen, *Mol. Phys.* **45**, 413 (1982).

<sup>42</sup> J. W. Greis, Ph.D. thesis, Universität Stuttgart, 1992.

<sup>43</sup> R. Speer, Diplomarbeit, Universität Stuttgart, 1988.

<sup>44</sup> C. A. Hutchison, Jr., J. V. Nicholas, and G. W. Scott, *J. Chem. Phys.* **53**, 1906 (1970).

<sup>45</sup> C. B. Harris and M. J. Buckley, in *Advances in Nuclear Quadrupole Resonance*, edited by J. A. Smith (Heyden, London, 1975), Vol. 2, p. 15.

<sup>46</sup> W. R. Leenstra and K. Vinodgopal, *Chem. Phys. Lett.* **115**, 311 (1985).

<sup>47</sup> F. Lenzian, H. van Willigen, S. Sastry, K. Möbius, H. Scheer, and R. Feick, *Chem. Phys. Lett.* **118**, 145 (1985).

<sup>48</sup> A. de Groot, R. Evelo, A. J. Hoff, R. de Beer, and H. Scheer, *Chem. Phys. Lett.* **118**, 48 (1985).

<sup>49</sup> H. Käss, J. Rautter, W. Zweggarth, H. Struck, H. Scheer, and W. Lubitz, *J. Phys. Chem.* **98**, 354 (1994).

<sup>50</sup> J. R. Norris, D. E. Budil, P. Gast, C.-H. Chang, O. El-Kabbani, and M. Schiffer, *Proc. Natl. Acad. Sci. USA* **86**, 4335 (1989).

<sup>51</sup> E. J. Lous and A. J. Hoff, *Proc. Natl. Acad. Sci. USA* **84**, 6147 (1987).

<sup>52</sup> O. El-Kabbani, C.-H. Chang, D. Tiede, J. R. Norris, and M. Schiffer, *Biochem. J.* **30**, 5361 (1991).

<sup>53</sup> I. H. Davis, P. Heathcote, D. J. MacLachlan, and M. C. W. Evans, *Biochim. Biophys. Acta* **1143**, 183 (1993).

<sup>54</sup> F. Lenzian, W. Lubitz, H. Scheer, A. J. Hoff, M. Plato, E. Tränkle, and K. Möbius, *Chem. Phys. Lett.* **148**, 377 (1988).

- <sup>55</sup>M. Plato, W. Lubitz, F. Lenzian, and K. Möbius, *Isr. J. Chem.* **28**, 109 (1988).
- <sup>56</sup>F. Lenzian, B. Bönigk, M. Plato, K. Möbius, and W. Lubitz, *NATO ASI Ser. A* **237**, 89 (1992); Proceedings of a NATO Advanced Research Workshop on The Photosynthetic Bacterial Reaction Center: Structure, Spectroscopy, and Dynamics, held May 10–15, 1992, at the Centre d'Etudes Nucléaires de Cadarache, France.
- <sup>57</sup>M. Plato, F. Lenzian, W. Lubitz, and K. Möbius, *NATO ASI Ser. A* **237**, 109 (1992); Proceedings of a NATO Advanced Research Workshop on The Photosynthetic Bacterial Reaction Center: Structure, Spectroscopy, and Dynamics, held May 10–15, 1992, at the Centre d'Etudes Nucléaires de Cadarache, France.
- <sup>58</sup>F. Lenzian, M. Huber, R. A. Isaacson, B. Endeward, M. Plato, B. Bönigk, K. Möbius, W. Lubitz, and G. Feher, *Biochim. Biophys. Acta* **1183**, 139 (1993).
- <sup>59</sup>G. L. Closs, P. Piotrowiak, J. A. MacInnis, and G. R. Fleming, *J. Am. Chem. Soc.* **110**, 2652 (1988).
- <sup>60</sup>R. G. Larsen, G. J. Gerfen, and D. J. Singel, *Appl. Magn. Reson.* **3**, 369 (1992).